# NON-LINEAR SECTIONAL ANALYSIS OF REINFORCED CONCRETE COLUMN STRENGTHENED BY REINFORCED CONCRETE JACKETING WITH HIGH-STRENGTH STEEL

Imron Imron[a], Bambang Piscesa[b*], Achfas Zacoeb[c]

***Abstract**: This paper presents a nonlinear sectional analysis of reinforced concrete (RC) columns strengthened by RC jacketing, which also utilizes a high-strength reinforcing bar. A simple interface slip model was used to model the relationship between the old and the new concrete material. The initial axial load and bending moment are included in the analysis by introducing an initially prescribed strain before loading. The nonlinear sectional analysis was performed using an in-house MATLAB code utilizing the fiber-based method. The RC section was discretized with constant strain triangles (CST). The developed RC column model with jacketing was validated using the available test results in the literature. After the validation of the model was completed, the parametric study was carried out to gain an insight into the effect of using high strength reinforcing bar in the jacket structural element. The curvature and $I_{10}$ ductility index were evaluated based on pure axial and constant axial loads with increased bending moment. From the validation of the model with the test result, the model predictions were satisfactorily showing a good fit, concluding that the developed MATLAB code can be used to evaluate RC columns strengthened with concrete jacketing. For the parametric study, the high strength reinforcing bar in RC column jacketing can increase the flexural, axial, and lateral load capacity but reduce the overall ductility. On the other hand, utilizing only high strength reinforcing bar for transverse reinforcement with tighter spacing resulted in higher ductility than if all the reinforcing bar was made from a high-strength one.*

**Keywords:** *Fiber-based method, interface slip, initial strain, high strength reinforcing bar, moment-curvature*

Submitted: 15 July 2022; Revised: 20 December 2022; Accepted: 20 December 2022

## INTRODUCTION

Earthquakes have caused many casualties, failures, and significant damage to the building infrastructure. The rehabilitation cost of building structures can be very expensive. Many buildings that were designed using outdated building codes or being built with non-code compliance can be very vulnerable when exposed to moderate to large earthquakes. In most cases, the casualties come from a low-rise building that is not compliant with the building codes. Therefore, significant effort to check the safety and function of the building must be carried out and strengthening might be needed to ensure the performance of the building satisfies the code requirements.

In most cases, the part that needed to be strengthened is the RC column. Failure of the RC column directly impacts the overall stability and strength of the building structure. The failure of the RC column can be caused by insufficient detailing which may result in insufficient ductility, and inadequate strength [1] (shear and flexure). Some methods are commonly used to retrofit RC columns such as RC jacketing, steel jacketing, and fiber-reinforced polymer (FRP) jacketing [2]. Among all the methods to retrofit RC columns, RC jacketing was one of the most practical methods: enlarging the cross section and providing a layer of reinforced concrete jacketing around the perimeter of the existing RC column [2-6].

[a]Master Student in the Civil Engineering Department, Institut Teknologi Sepuluh Nopember, ITS Campus, Sukolilo, Surabaya 60111, Indonesia
[b]Lecturer in the Civil Engineering Department, Institut Teknologi Sepuluh Nopember, ITS Campus, Sukolilo, Surabaya 60111, Indonesia. Corresponding author email address: piscesa@ce.its.ac.id
[c]Department of Civil Engineering, Faculty of Engineering, University of Brawijaya, Malang 68121, Indonesia

The efficiency of RC jacketing depends on the surface interaction between the core and the jacket concrete. When there exists friction (either from surface roughness or the existence of the shear connectors), the jacket structure can carry some axial and lateral loads. On the other hand, if the friction was neglected, the jacket structure only acts as confining device that confined the concrete core. From the previous research works, the use of the jacketing method can increase the strengths (flexural, shear, and axial strengths) of the retrofitted RC column, provide higher stiffness, and improve ductility [2, 4-7]. Treatment of the interface can also affect the strength and rigidity of the column. From past researchers, the surface treatment using sandblasting showed to be the best [4, 5].

In ACI 318-19 [8], The use of the high-strength reinforcing bar, which was based on ASTM 615 [9] and ASTM 706 [10], was permitted to be used for transverse steel reinforcement in a special seismic resisting system. With the use of these high-strength steel reinforcing bars, the diameter for the confining bar can be significantly reduced and thus increases the workability of concrete during casting due to larger pitch spacing between the transverse bars. Considering the benefit of using high-strength rebar, in this study, the capacity of RC columns strengthened with RC jacketing made of high-strength rebar is being examined thoroughly.

## RESEARCH SIGNIFICANCE

This paper investigates the performance of RC columns retrofitted with RC jacketing using both normal- and high-strength reinforcing bars. Nonlinear sectional analysis was carried out using the fiber-based method with different confining pressure for each layer of the section. The model was verified with existing experimental data available in the literature. Curvature ductility and $I_{10}$ ductility index were used for the ductility measurement of the retrofitted RC column.

## METHODOLOGY

The research methodology in this paper is divided into four stages which are: 1) Input data preparation for geometry and material of the RC core and jacket. At this stage, both the verification model and parametric model were prepared for validation and further insight into the performance of the model. 2) Establish a fiber-based model for nonlinear cross-sectional analysis. 3) Evaluation of the constitutive model for each material. 4) Confining pressure estimation from the governing sectional equilibrium in the transverse direction. 5) Ductility measures evaluation of the modeled specimen using curvature ductility and $I_{10}$ ductility index.

### A. INPUT DATA FOR GEOMETRY AND MATERIAL PROPERTIES

The general geometry for the RC column retrofitted with the RC jacket consists of an additional casting layer of RC around the existing RC column as shown in Figure 1. The definition for each notation can be found in the notation list section at the end of the paper. It should be noted that the steel reinforcement properties for the reinforced concrete (RC) core and jacket sections were possibly to be not similar. Therefore, the notation for the reinforcing bar for both sections was differentiated. The definition of the concrete core section comprises the concrete cover and the concrete core of the RC core section.

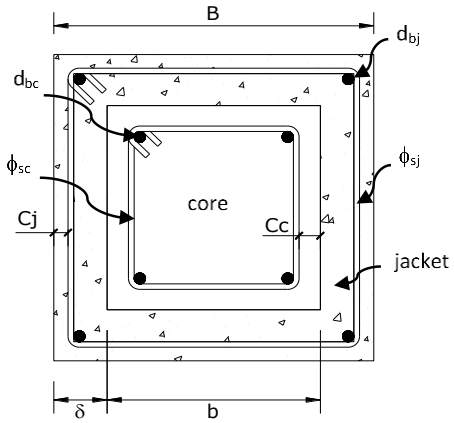


Figure 1 Geometry of RC section reinforced with a reinforced concrete jacket

Table 1 and Table 2 show the input geometry and material properties for the RC core and jacket sections with different types of jacket retrofitting, respectively. The type of RC columns strengthening are classified as Monolithic (MBR), Repaired (RBR), and Strengthened (SBR). For type M RC columns, the concrete strength was similar for both the core and jacket sections. For types R and S, the concrete compressive strength of the jacket section was higher than the core section. The difference between the R and S type was in the initially applied loading to the concrete core section. For type R, the core was loaded until the core was damaged and slight buckling in the longitudinal bar was seen. The RC column was then repaired and jacketed. For type S, the core was loaded until it reached 75% of its axial load capacity and the load was released. Type R is considered the damaged RC column and while Type S is considered the undamaged RC column.

Table 1 Input geometry and material properties for the RC core section

| Type | $b$ | $c_c$ | $d_{bc}$ | $\phi_{sc}$ | $f_{cco}$ | $f_{yco}$ | $f_{ysco}$ |
|---|---|---|---|---|---|---|---|
| MBR | 160 | 5 | 4Ø12 | Ø4-100 | 31.5 | 300 | 300 |
| RBR | 160 | 5 | 4Ø12 | Ø4-100 | 30.7 | 300 | 300 |
| SBR | 160 | 5 | 4Ø12 | Ø4-100 | 33 | 300 | 300 |

Table 2 Input geometry and material properties for the RC jacket section

| Type | $\delta$ | $c_j$ | $d_{bj}$ | $\phi_{sj}$ | $f_{cj}$ | $f_{yj}$ | $f_{ysj}$ |
|---|---|---|---|---|---|---|---|
| MBR | 35 | 5 | 4Ø12 | Ø8-100 | 31.5 | 280 | 280 |
| RBR | 35 | 5 | 4Ø12 | Ø8-100 | 34.5 | 280 | 280 |
| SBR | 35 | 5 | 4Ø12 | Ø8-100 | 40.3 | 280 | 280 |

### B. FIBER-BASED MODEL FOR NON-LINEAR CROSS-SECTIONAL ANALYSIS

The fiber-based model was used to evaluate the nonlinear response of the RC column. The MATLAB program is used for the implementation of the model [11, 12]. The cross-section was meshed using the constant-strain triangle (CST) element type [13]. Figure 2 showed the modeled sectional analysis which was based on the available test result [14]. The longitudinal bar was modeled as nodes and represented as blue and red circles in Figure 2.

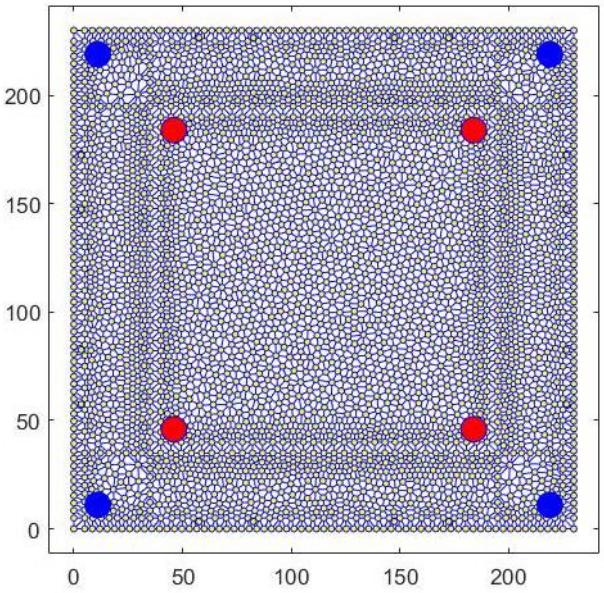


Figure 2 Cross-sectional meshed RC column strengthened with RC jacket

The axial force (F) and bending moment ($M_{yy}$ and $M_{xx}$) of the cross-section can be computed as follows:

$$F = \sum_{i=1}^{n_{ele}} \sigma_i A_i \tag{1}$$

$$M_{yy} = \sum_{i=1}^{n_{ele}} \sigma_i A_i \left( x_i - \overline{x} \right) \tag{2}$$

$$M_{xx} = \sum_{i=1}^{n_{ele}} \sigma_i A_i \left( y_i - \overline{y} \right) \tag{3}$$

### C. CONSTITUTIVE MODEL OF MATERIALS

The constitutive model for both unconfined and confined concrete was based on the Attard and Setunge model [7] which works well with 20 to 130 MPa concrete strength.

The model of [7] works by computing the stress with a given axial strain. The general expression for the stress-strain relationship is given by:

$$Y = \frac{AX + BX^2}{1 + CX + DX^2} \tag{4}$$

$$Y = \frac{f}{f_0} \quad X = \frac{\varepsilon}{\varepsilon_0} \quad \forall X \geq 0 \text{ and } 0 \leq Y \leq 1 \tag{5}$$

The expression for the axial peak stress for unconfined and confined concrete ($f_o$) is:

$$\frac{f_0}{f_c^{'}} = \left( \frac{f_r}{f_t} + 1 \right)^k \tag{6}$$

$$k = 1.25 \left[ 1 + 0.062 \frac{f_r}{f_c^{'}} \right] \left( f_c^{'} \right)^{-0.21} \tag{7}$$

It should be noted that the concrete capacity in tension is assumed to be zero. The constitutive model for the steel reinforcing bar is using bilinear stress-strain model with and without hardening [15].

## D. CONFINING PRESSURES

The confining pressure for the RC jacketed column should be evaluated for the core and the jacket components. Each of the components has its mechanism, but it is possible to evaluate the mechanism individually and combining them later. Figure 3 shows the RC column section that is being cut to see the tensile forces and the confining pressures that act on the section.

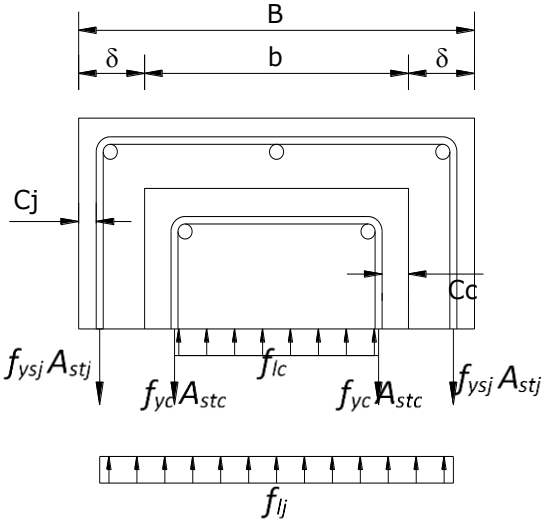


Figure 3 Confinement pressure in the core and jacket

Balancing the tensile forces with the confining pressures times the length of the confined section and the pitch spacing of the confining rebar [16, 17] which was originally from [1], the expression for both the confining pressures ($f_{lc}$ and $f_{lj}$) can be expressed as:

$$f_{lc} = \frac{2 f_{y,st,co} A_{st,co}}{(b - c) s_c} \tag{8}$$

$$f_{lj} = \frac{2 f_{y,st,j} A_{st,j}}{(B - \delta) s_j} \tag{9}$$

The coefficient of the confinement effectiveness due to the jacket influence for both in x and y directions ($k_{ej}$ and $k_{vj}$) is determined by the following equation:

$$k_{ej} = 1 - \frac{2}{3b^2} \sqrt{\left(b + 2c_j - 2\delta\right)^3} \sqrt{b - 2c_j + 2\delta} \tag{10}$$

$$k_{vj} = \left( 1 - \frac{s_j}{2\left(b + 2\delta - 2c_j\right)} \right)^2 \tag{11}$$

## E. MEASUREMENT OF DUCTILITY

The measurement of ductility was carried out using both the curvature ductility ($\mu$) and the $I_{10}$ index ductility.

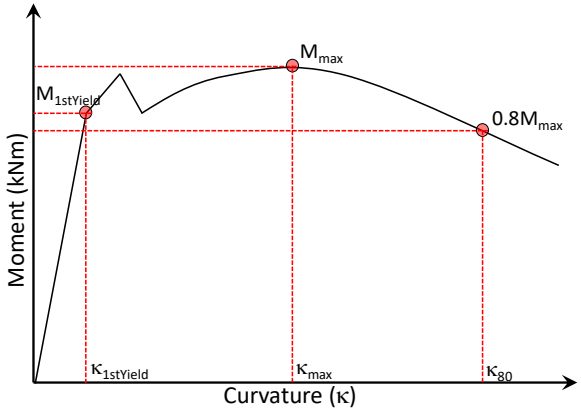


Figure 4 The moment-curvature relationship

The curvature ductility of the RC column is usually determined using the moment-curvature relationship of the cross-section. The curvature itself is known as the rotation per unit length of the element and is used to determine the rotational capacity of the section. Figure 4 shows the typical moment-curvature relationship which clearly shows the position of the maximum bending moment ($M_{100}$), 80 % bending moment capacity ($M_{80}$) which relates to the ultimate curvature of the column ($\varphi_u$), and the curvature of the section when the reinforcing steel yield ($\varphi_y$). The ductility of the section ($\mu$) is measured by taking the ratio of the ultimate to the yield curvature and is:

$$\mu = \frac{\varphi_u}{\varphi_y} \tag{12}$$

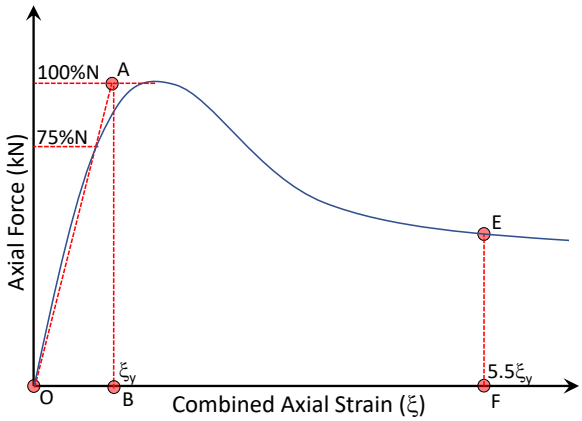


Figure 5 The axial load as a function of the combined nominal strain ($\xi$) curve

The $I_{10}$ ductility index, on the other hand, is the parameter that defines the ductility of the column using the absorbed energy measured at 5.5 times the nominal yield strain. The $I_{10}$ ductility index can be computed as a function of the average strain ($\varepsilon_{avg}$), the curvature ($\kappa$), and the eccentricity ($e$) and is:

$$\xi = \varepsilon_{avg} + \kappa e \quad (12)$$

Figure 5 shows the $I_{10}$ ductility index as proposed by Foster and Attard [18]. The $I_{10}$ ductility index is defined as the area of OEF divided by the area of OAB.

F. STRAIN COMPATIBILITY

The slip between the old and the new concretes should be considered in the analysis. Figure 6 shows the strain compatibility of the section for the RC jacketed column [19]. The slip factor (η) was introduced to simulate the slip that occurs between the old and the new concretes by scaling the corresponding strain such that the strain was incompatible which clearly shows slips occurred. For the monolithic case, the value for n is unity. For the non-monolithic case, the mechanism of sliding resistance is obtained from the aggregate interlock between the contact surface of the core and jacket including the initial bond from the jacket concrete. When shear friction reinforcement is present, the friction influence which works normally with the interface and the dowel action should be considered in the analysis.

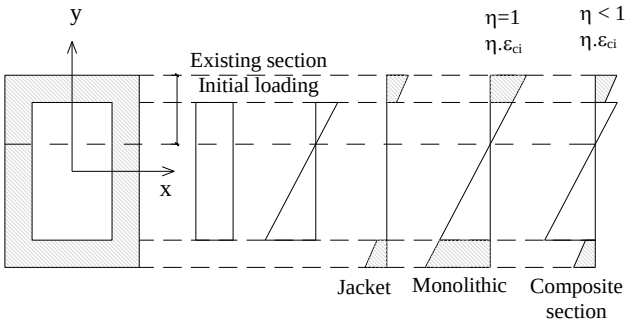


Figure 6 Strain compatibility of the RC jacketed column

For the non-monolithic case, the slip factor should be used to estimate the reduced strain due to slip. Therefore, the slip factor value should be between 0 and 1. A value of slip factor 0 shows that there is no bond at all while a value of 1 assumes that a perfect bond occurred and therefore the strain is fully compatible as in the monolithic case. Caglar et al., 2020 [20] proposed that the value of the interface slip coefficient ($\eta$) for various treatments on the interface ranges from 0.75 – 1, depending on the method used for treatment, as shown in Table 2.

Table 2 Interface slip coefficient ($\eta$)

| Type of Treatment | Interface slip coefficient ($\eta$) |
|---|---|
| No-treatment | 0.75 |
| Dowel / Steel Connector | 0.8-0.85 |
| Roughness | 0.85-0.9 |
| Roughness and dowel | 0.9 |

If the initial load in the existing column is present, an initial strain can be imposed into the section to represent the effect of the initial load on the section. The non-linear analysis of the RC with the jacket that considers the initial loading in the existing column is calculated by modifying the strain value in the existing section (core). This strain value in the existing section must be added to the initial strain, while the initial strain is not added to the jacket section.

## ANALYSIS RESULTS AND DISCUSSIONS

Three jacketed RC columns tested by [14] will be evaluated using non-linear fiber-based analysis. The relationship that is being investigated and compared is localized only to the moment-curvature analysis. The specimen geometry is reported in Table 1, and the concrete compressive strength was varied for each case. The first specimen is identified as MBR which represents the monolithic connection between the concrete core and the jacket. Before applying lateral load, a constant axial load of 630 kN was given. The second specimen (RBR) which considers concrete crushing before strengthening is given a constant axial load of 620 kN before the lateral load sequence. The third and last specimen (SBR) is firstly loaded until the concrete cover of the concrete core spalls, strengthened with RC jacketing, and is given a constant axial load of 635 kN before the lateral load procedure commended.

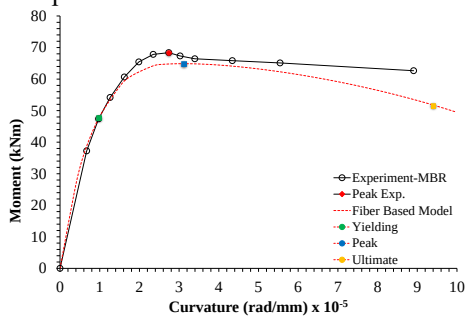


(a)

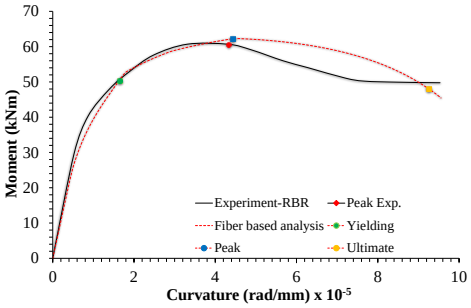


(b)

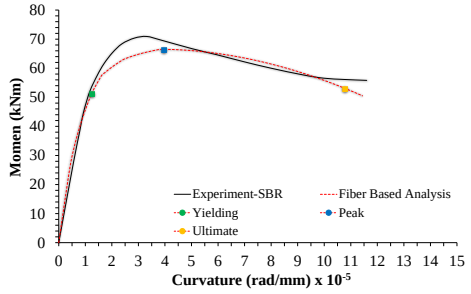


(c)

Figure 7 Comparison of the proposed model with the test result (a) MBR column, (b) RBR column, (c) SBR column

Figure 7 shows the comparison of the proposed model with the available test results for MBR, RBR, and SBR columns. As shown in Figure 7, the performance of the proposed model was sufficient to predict the behavior of the jacketed RC column with varying initial conditions.

Table 3 Moment-curvature comparison between the experimental data and the proposed model

| Specimens | Experimental Data | | Proposed Model | |
|---|---|---|---|---|
| | $M_{max}$ (kN.m) | $\varphi_{max}$ (rad/m) | $M_{max}$ (kN.m) | $\varphi_{max}$ (rad/m) |
| MBR | 71.1 | 0.040 | 64.87 | 0.0311 |
| RBR | 65.9 | 0.038 | 61.56 | 0.0343 |
| SBR | 73.2 | 0.033 | 66.96 | 0.0374 |

The input values for the interface slip coefficient for specimen MBR, RBR, and SBR were set to 1.0, 0.75, and 0.90, respectively.

Table 4 Variation model with HSS reinforcement

| Model | $d_{bj}$ (mm) | $f_{y,j}$ (MPa) | $\varnothing_{sj}$ (mm) | $f_{ys,j}$ (MPa) |
|---|---|---|---|---|
| MBR-RBR-SBR | 4Ø12 | 280 | Ø8-100 | 280 |
| Var-1 | 4Ø12 | 280 | Ø4-60 | 690 |
| Var-2 | 4Ø12 | 280 | Ø5-100 | 690 |
| Var-3 | 4Ø8 | 690 | Ø5-100 | 690 |
| Var-4 | 4Ø8 | 690 | Ø8-100 | 280 |
| Var-5 | 4Ø8 | 690 | Ø4-60 | 690 |

Table 4 shows the variation of reinforcing details in the available tested specimen (MBR/RBR/SBR) and the model for parametric study. The parametric study of the RC jacketed RC column with high-strength steel reinforcement (HSSR) was carried out with different longitudinal and transverse reinforcement, as well as the reinforcement diameter and pitch spacing. Table 5 shows the moment and curvature at yield, maximum, and ultimate conditions. As shown in Table 5, the bending moment capacity at yield for MBR was lower than RBR and SBR overall except for RBR-3, RBR-4, and RBR-5 were typically similar. At maximum load, the bending moment capacity for MBR, RBR, and SBR was somewhat similar. This is possible when the capacity at maximum load was controlled by the longitudinal reinforcing bar. The contribution from the concrete was not significant. At the ultimate condition, measured when the moment capacity drops to 80 % of its peak capacity, the moment capacity for MBR was greater than RBR but lower than SBR.

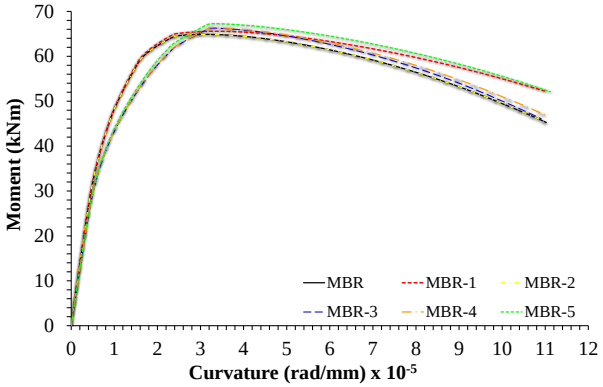


Figure 8 Moment-curvature of variation models for MBR type specimen

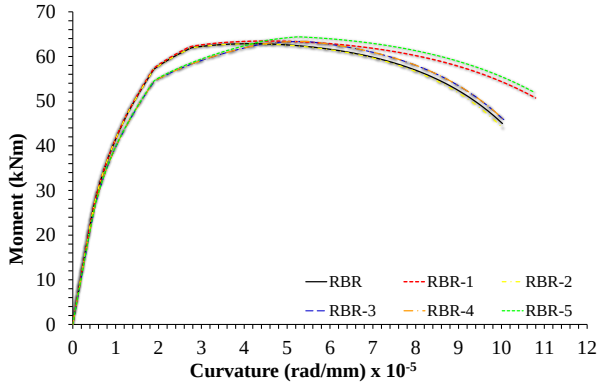


Figure 9 Moment-curvature of variation models for RBR type specimen

Table 5 Results of moment-curvature model variations of MBR, RBR, SBR

| Model | $M_{yield}$ (kN.m) | $M_{max}$ (kN.m) | $M_{ultimate}$ (kN.m) | $\varphi_{yield}$ (rad/mm) x $10^{-5}$ | $\varphi_{max}$ (rad/mm) x $10^{-5}$ | $\varphi_{ultimate}$ (rad/mm) x $10^{-5}$ |
|---|---|---|---|---|---|---|
| MBR | 47.71 | 64.87 | 51.89 | 0.98 | 3.12 | 9.39 |
| MBR-1 | 47.92 | 65.56 | 52.45 | 0.97 | 3.38 | 10.96 |
| MBR-2 | 47.67 | 64.77 | 51.82 | 0.97 | 3.11 | 9.20 |
| MBR-3 | 56.95 | 66.28 | 53.02 | 1.89 | 3.31 | 9.31 |
| MBR-4 | 57.02 | 66.39 | 53.11 | 1.90 | 3.22 | 9.50 |
| MBR-5 | 57.56 | 67.10 | 53.68 | 1.91 | 3.38 | 11.07 |
| RBR | 51.71 | 62.67 | 50.14 | 1.89 | 4.71 | 9.70 |
| RBR-1 | 51.72 | 62.72 | 50.17 | 1.89 | 4.72 | 9.80 |
| RBR-2 | 51.71 | 62.68 | 50.14 | 1.89 | 4.71 | 9.71 |
| RBR-3 | 56.56 | 61.96 | 49.57 | 2.73 | 6.18 | 9.78 |
| RBR-4 | 56.59 | 62.07 | 49.65 | 2.73 | 6.19 | 9.93 |
| RBR-5 | 56.60 | 62.15 | 49.72 | 2.74 | 6.28 | 10.0 |
| SBR | 53.07 | 66.49 | 53.19 | 1.33 | 3.95 | 10.77 |
| SBR-1 | 53.27 | 67.06 | 53.65 | 1.34 | 4.23 | 12.56 |
| SBR-2 | 53.04 | 66.40 | 53.12 | 1.33 | 3.94 | 10.57 |
| SBR-3 | 66.10 | 67.86 | 54.29 | 3.25 | 4.36 | 10.70 |
| SBR-4 | 66.16 | 67.96 | 54.36 | 3.26 | 4.37 | 10.86 |
| SBR-5 | 66.55 | 68.60 | 55.14 | 3.30 | 4.45 | 12.66 |

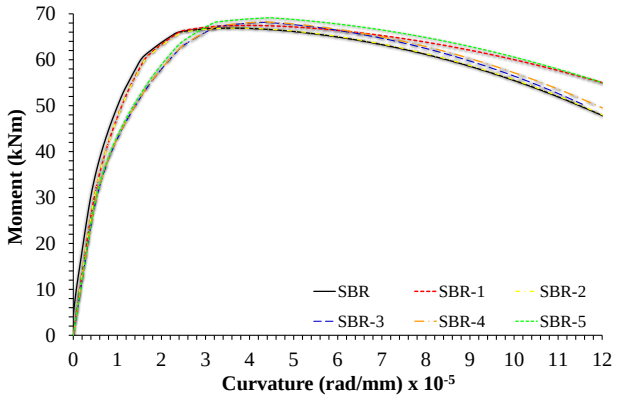


Figure 10 Moment-curvature of variation models for SBR

The curvature at yield and at maximum, for RBR and SBR, was improved quite significantly compared to MBR. The anomaly was found for SBR, SBR-1, and SBR-2 specimens where the curvature values were lower than the RBR specimens which might be caused by the larger initial stiffness for the SBR specimen. Another interesting finding is that the ultimate curvature for MBR and RBR specimens was found to be identical. In contrast with the SBR specimen, the ultimate curvature was improved compared to the MBR specimen. At ultimate condition, the curvature ultimate for MBR and RBR specimens were similar. On the other hand, the curvature ultimate for SBR performed the best.

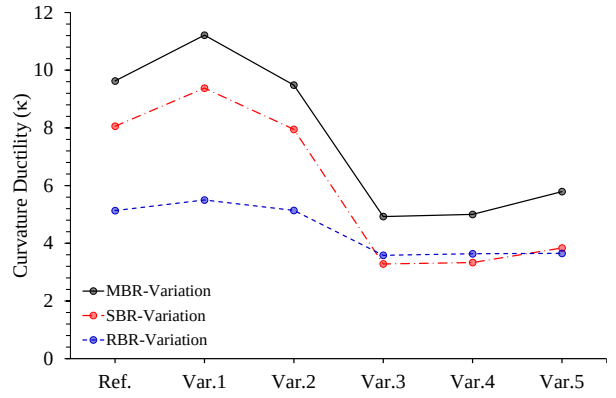


(a)

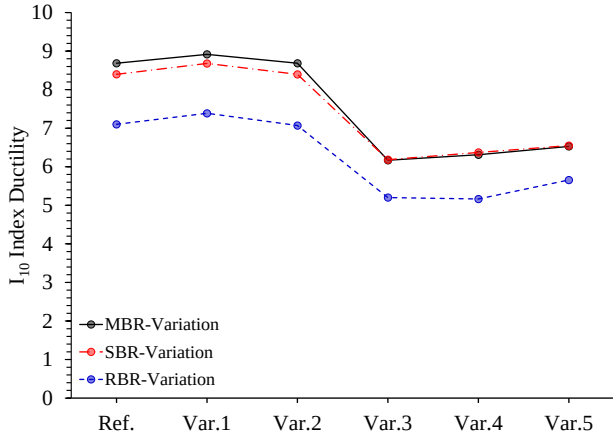


(b)

Figure 11 (a) Curvature ductility, (b) $I_{10}$ ductility index

Figure 8, Figure 9, and Figure 10 show the plots for the moment-curvature relationship for each of the modeled specimens. As shown in those figures, the initial stiffness for each variation was similar but start to deviate when the columns were in the inelastic stages. Once the peak moment is reached, the moment capacity degrades and resulted in two softening paths for most of the modeled variations.

Figure 11 shows the plot for the computed curvature ductility and $I_{10}$ ductility index, respectively. As shown in Figure 11, the performance of the RBR specimen was found to be the worst followed by the SBR specimen. MBR specimens perform the best of the curvature ductility. The anomaly was found in the SBR specimen with Var-3, Var-4, and Var-5 where the curvature ductility index was slightly lower than in the RBR specimen.

Almost similar finding with the curvature ductility, the $I_{10}$ ductility index for RBR performs the worst followed by the SBR specimen. However, unlike the curvature ductility value, the value for the $I_{10}$ ductility index for SBR with Var-3, Var-4, and Var-5 specimens was coincide with the MBR specimen. This finding noted that the $I_{10}$ ductility index was more reasonable to be used compared to the curvature ductility since the logic that the SBR specimen should perform better than the SBR specimen was expected.

## CONCLUSIONS

This paper has presented the ductility level of RC column reinforced with RC Jacket evaluated using the nonlinear sectional fiber-based model. Both the curvature ductility and $I_{10}$ ductility index were used to evaluate the ductility level of the RC column. The HSS rebar reinforcement was designed based on the ACI 318-19 and was regulated for its use in special seismic systems. The analysis results showed that the proposed model can well predict the response of the jacketed RC column.

From the study, the use of the jacketed method to repair a damaged RC column can be successful despite the level of damage given to the existing RC column. The interface slip coefficient which reflects the surface treatment plays an important role to enhance not only the strength but also the ductility of the jacketed RC column.

The use of high-strength steel reinforcing bars (HSSR) can increase the flexure, axial, and lateral load capacity but may result in lower ductility. On the other hand, the use of normal-strength steel reinforcing bar for the longitudinal bar and using HSSR for the confinement with tighter pitch spacing can produce higher ductility compared to the experiment.

## REFERENCES

[1] J. B. Mander, M. J. Priestley, and R. Park, "Theoretical stress-strain model for confined concrete," Journal of Structural Engineering, vol. 114, no. 8, pp. 1804-1826, 1988.

[2] A. R. Takeuti, J. B. de Hanai, and A. Mirmiran, "Preloaded RC columns strengthened with high-strength concrete jackets under uniaxial compression," Materials and Structures, vol. 41, no. 7, pp. 1251-1262, 2008.

[3] K. Ong, Y. Kog, C. Yu, and A. Sreekanth, "Jacketing of reinforced concrete columns subjected to axial load," Magazine of Concrete Research, vol. 56, no. 2, pp. 89-98, 2004.

[4] S. N. Bousias, D. Biskinis, M. N. Fardis, and A.-L. Spathis, "Strength, stiffness, and cyclic deformation capacity of concrete jacketed members," ACI Structural Journal, vol. 104, no. 5, p. 521, 2007.

[5] E. Júlio and F. A. Branco, "Reinforced concrete jacketing-interface influence on cyclic loading response," ACI Structural Journal, vol. 105, no. 4, p. 471, 2008.

[6] K. G. Vandoros, and S. E. Dritsos, "Concrete jacket construction detail effectiveness when strengthening RC columns," Construction and Building Materials, vol. 22, no. 3, pp. 264-276, 2008.

[7] M. Attard, and S. Setunge, "Stress-strain relationship of confined and unconfined concrete," ACI Materials Journal, vol. 93, no. 5, 1996.

[8] A. C. I. Committee, Building code requirements for structural concrete (ACI 318-19) and commentary, (Farmington Hills: American Concrete Institute), 2019.

[9] A. S. T. Materials, ASTM A615/A615M-09b Standard specification for deformed and plain carbon-steel bars for concrete reinforcement, 2009.

[10] A. S. T. Materials, ASTM A706/A706M–04a Standard specification for low-alloy steel deformed and plain bars for concrete reinforcement, 2009.

[11] B. Piscesa, M. Attard, P. Suprobo, and A. Samani, "Investigation on the fiber based approach to estimate the axial load carrying capacity of the circular concrete filled steel tube (CFST)," in IOP Conference Series: Materials Science and Engineering, 2017, vol. 267, no. 1: IOP Publishing, p. 012017.

[12] B. Piscesa, D. Prasetya, M. Irmawan, and H. Alrasyid, "Ductility evaluation of reinforced concrete column made of normal- to high-strength concrete under constant axial load level combined with flexural loading using nonlinear sectional fiber based model," Journal of Civil Engineering, vol. 34, no. 1, pp. 3-8, 2019.

[13] D. L. Logan, A first course in the finite element method. Cengage Learning, 2016.

[14] U. Ersoy, A. T. Tankut, and R. Suleiman, "Behavior of jacketed columns," Structural Journal, vol. 90, no. 3, pp. 288-293, 1993.

[15] R. Park, and T. Paulay, Reinforced concrete structures. John Wiley & Sons, 1975.

[16] G. Campione, M. Fossetti, C. Giacchino, and G. Minafò, "RC columns externally strengthened with RC jackets," Materials and Structures, vol. 47, no. 10, pp. 1715-1728, 2014.

[17] G. Minafò, F. Di Trapani, and G. Amato, "Strength and ductility of RC jacketed columns: A simplified analytical method," Engineering Structures, vol. 122, pp. 184-195, 2016.

[18] S. J. Foster, and M. M. Attard, "Experimental tests on eccentrically loaded high strength concrete columns," Structural Journal, vol. 94, no. 3, pp. 295-303, 1997.

[19] G. E. Thermou, V. K. Papanikolaou, and A. J. Kappos, "Flexural behaviour of reinforced concrete jacketed columns under reversed cyclic loading," Engineering Structures, vol. 76, pp. 270-282, 2014.

[20] N. Caglar, A. Sichko, H. Sezen, E. Bicici, A. Demir, and A. F. Farah, "Interface slip model for reinforced concrete columns strengthened with concrete jacketing," Revista de la Construcción, vol. 19, no. 2, pp. 180-189, 2020.

## LIST OF NOTATIONS

$b$ is the width of the existing RC column (mm)
$c_c$ is the cover thickness of the column existing (mm)
$\delta$ is the concrete jacket thickness (mm)
$c_j$ is the cover thickness of the concrete jacket (mm)
$d_{bc}$ is the diameter and number of the longitudinal bar for the core section (mm)
$\phi_{sc}$ is the diameter and spacing of the transverse bar for the core section (mm)
$f_{cco}$ is the concrete compressive strength for the concrete core section (MPa)
$f_{yco}$ is the longitudinal steel yield strength of the concrete core section (MPa)
$f_{ysco}$ is the transverse steel yield strength of the concrete core section (MPa)
$d_{bj}$ is the number and diameter of the longitudinal steel rebar of the jacket section (mm)
$\phi_{sj}$ is the diameter and spacing of the transverse steel rebar of jacket section (mm)
$f_{cj}$ is the concrete compressive strength of jacket section (MPa)
$f_{yj}$ is the longitudinal steel yield strength of jacket section (MPa)
$f_{ysj}$ is the transverse steel yield strength of jacket section (MPa)
$F$ is the axial force capacity of the cross section (N or kN)
$M_{xx}$ is the bending moment capacity of the cross section with respect to the x-axis (Nmm or kNm)
$M_{yy}$ is the bending moment capacity of the cross section with respect to the y-axis (Nmm or kNm)
$\sigma_i$ is the axial stress of the $i^{th}$ element (MPa)
$A_i$ is the area of of the $i^{th}$ element (mm)

$y_i$ is the centroid of each element in y direction (mm)
$x_i$ is the centroid of each element in x direction (mm)
$\bar{x}$ is the centroid of the section in x direction (mm)
$\bar{y}$ is the centroid of the section in y direction (mm)
$n_{ele}$ is the total number of elements
$f$ is the axial stress (MPa)
$f_o$ is the axial stress when the axial strain is equal to the axial strain at peak (MPa)
$\varepsilon$ is the axial strain
$\varepsilon_0$ is the axial strain at peak stress
A, B, C and D are constants which depend on the boundary condition (see Attard and Setunge [5])
$f_r$ is the confining pressure (MPa)
$f_t$ is the concrete uniaxial tensile strength (MPa)
$f_{lc}$ is the confinement pressure of the concrete core (MPa)
$f_{lj}$ is the confinement pressure of the concrete jacket (MPa)
$f_{y,st,co}$ is the yield strength of the transverse rebar for the concrete core (MPa)
$f_{y,st,j}$ is the yield strength of the transverse rebar for the concrete jacket (MPa)
$A_{st,co}$ is the area of the confining bar for the core section
$A_{st,j}$ is the area of the confining bar for the jacket section
$N$ is the axial load
$\varepsilon_{avg}$ is the average strain
$\varepsilon$ is the load eccentricity
$\kappa$ is the curvature